Conditional Spin Squeezing of a Large Ensemble via the Vacuum Rabi Splitting

Zilong Chen, Justin G. Bohnet, Shannon R. Sankar, Jiayan Dai, and James K. Thompson

JILA, NIST, and Department of Physics, University of Colorado, Boulder, Colorado 80309-0440, USA

(Received 11 August 2010; revised manuscript received 10 December 2010; published 29 March 2011)

We use the vacuum Rabi splitting to perform quantum nondemolition measurements that prepare a conditionally spin squeezed state of a collective atomic psuedospin. We infer a 3.4(6) dB improvement in quantum phase estimation relative to the standard quantum limit for a coherent spin state composed of uncorrelated atoms. The measured collective spin is composed of the two-level clock states of nearly 10^6 ^{87}Rb atoms confined inside a low finesse $F = 710$ optical cavity. This technique may improve atomic sensor precision and/or bandwidth, and may lead to more precise tests of fundamental physics.

DOI: 10.1103/PhysRevLett.106.133601 PACS numbers: 42.50.Pq, 03.65.Yz, 37.30.+i, 42.50.Dv

Large ensembles of uncorrelated atoms are extensively used as precise sensors of time, rotation, and gravity, and for tests of fundamental physics [1–4]. The quantum nature of the sensors imposes a limit on their ultimate precision. Large ensembles of N atoms can be used to average the quantum noise as $1/\sqrt{N}$, a scaling known as the standard quantum limit. However, the ensemble size is limited by both technical constraints and atom-atom collisions—a fundamental distinction from photon-based sensors. Learning to prepare entangled states of large ensembles with noise properties below the standard quantum limit will be key to extending both the precision [5] and/or bandwidth [6] of atomic sensors. More broadly, the generation and application of entanglement to solve problems is a core goal of quantum information science being pursued in both atomic and solid state systems.

In this Letter, we utilize the tools of cavity-QED to prepare an entangled ensemble with a 3.4(6) dB improvement in spectroscopic sensitivity over the standard quantum limit. The method does not require single particle addressability and is applied to a spectroscopically large ensemble of $N = 7 \times 10^5$ atoms using a single <200 μs operation. The gain in sensitivity is spectroscopically equivalent to the enhancement obtained had we created $>10^5$ pairs of maximally entangled qubits, demonstrating the power of a top-down approach for entangling large ensembles. The probing of atomic populations via the vacuum Rabi splitting is also of broad interest for nondestructively reading out a wide variety of both atomic and solid state qubits.

The large ensemble size is a crucial component. Entangled states of cold, neutral atoms are unlikely to impact the future of quantum sensors and tests of fundamental physics unless the techniques for generating the states are demonstrated to work for the 10^4 to 10^7 neutral atom ensembles typically used in primary frequency standards [7] and atom interferometers [2,4].

The approach described here allows quantum-noise limited readout of a sensor with <0.2 photon recoils/atom, producing little heating of the atomic ensemble. Applied to a state-of-the-art optical lattice clock, the resulting enhanced measurement rates will suppress the dominant aliasing of the local oscillator noise [1,8].

The gain in spectroscopic sensitivity demonstrated here is far from the fundamental Heisenberg limit which scales as $1/N$, a limit approached by creating nearly maximally entangled states of 2 to 14 ions [9–11]. However, the gain here relative to the standard quantum limit is comparable to these experiments. Ensembles of $N \approx 10^3$ atoms have been spin squeezed by exploiting atom-atom collisions within a Bose-Einstein condensate [12–14]; however, these systems face the significant challenge of managing systematic errors introduced by the required strong atomic interactions.

Spin squeezed states can also be prepared with atom-light interactions that generate effective long range interactions on demand. In the approach followed here [15], light is used to perform a measurement that projects the ensemble into a conditionally spin squeezed state, as shown for clock transitions with laser cooled atoms in free space (3.4 dB at $N = 1.2 \times 10^5$ [16]) and in a cavity (3.0 dB at $N = 3.3 \times 10^4$ [17]). Conditional two-mode squeezing of a room temperature vapor of $N = 10^{12}$ atoms enabled magnetometry with 1.5 dB of spectroscopic enhancement and an increased measurement bandwidth [18]. A nonlinear atom-cavity system also generated 5.6 dB of spin squeezing at $N = 3 \times 10^4$ atoms [19].

The work we present here is unique in that we probe the atomic ensemble in the on-resonance regime of strong collective coupling cavity-QED. By doing so, we hope to counter a commonly held view that the quality of a coherence-preserving quantum nondemolition (QND) measurement is fundamentally linked to the probe's large detuning from atomic resonance. Instead, it is the magnitude of the collective cooperativity parameter NC (equivalent to the optical depth for a free space experiment) that sets the fundamental quality of the QND measurement [6]. In the context of free space measurements, detuning from resonance creates little enhancement in sensitivity once the detuned optical depth falls below one. Using an optical

cavity to enhance the cooperativity parameter has the potential to allow similar results to free space experiments, but at atomic densities lowered by a factor of order the cavity finesse.

Each atom in the ensemble can be represented as a pseudospin-$\frac{1}{2}$, with the quantity to be measured (i.e., energy splitting, acceleration, etc.) represented by the magnitude of an effective magnetic field that causes the total spin or Bloch vector to precess [20]. Quantum mechanics sets a fundamental limit on our ability to measure the precession angle ϕ and hence infer the value of the effective magnetic field. For an ensemble of uncorrelated spins, the quantum phase uncertainty is $\Delta\phi = 1/\sqrt{N}$, and is referred to as the standard quantum limit for a coherent spin state (CSS). This uncertainty can be more generally visualized as a classical probability distribution of possible positions of the tip of a classical vector on the surface of a Bloch sphere, as shown in Fig. 1. This noise is equivalent to projection noise arising from measurement-induced collapse into spin up or down [20].

A quantum particle's position can be determined with unlimited precision at the expense of knowing its momentum. In direct analogy, we demonstrate QND measurements that reduce the uncertainty in the polar angle θ_B describing the Bloch vector, at the expense of quantum backaction appearing in the azimuthal angle ϕ_B.

A pseudospin-$\frac{1}{2}$ system is formed by the clock states $|\uparrow\rangle \equiv |F = 2, m_F = 0\rangle$ and $|\downarrow\rangle \equiv |F = 1, m_F = 0\rangle$ of ^{87}Rb [Fig. 2(a)]. The ensemble of N particles is described by a collective Bloch vector $\mathbf{J} = \sum_i \mathbf{j}_i$ ($\mathbf{j}_i$ is the spin of the ith particle). In the fully symmetric manifold, the Bloch vector has length $J = J_{\max} = N/2$ and $\langle \mathbf{J}^2 \rangle = J(J+1)$. The z component of the Bloch vector is proportional to the population difference between the $|\uparrow\rangle$ and $|\downarrow\rangle$ states, $J_z = (N_\uparrow - N_\downarrow)/2$. In our experiments, the Bloch vector is prepared through a combination of optical pumping and microwave induced rotations in the state $\langle \mathbf{J} \rangle = \hat{x}N/2$. The polar angle is determined by the measured populations $\theta_B \approx J_z/|\langle \mathbf{J} \rangle| = (N_\uparrow - N_\downarrow)/(2|\langle \mathbf{J} \rangle|)$. We show that reduced uncertainty states with respect to θ_B can be prepared by first demonstrating that J_z can be measured with precision better than the CSS noise $\Delta J_{z\mathrm{CSS}} = \sqrt{N}/2$, and then by demonstrating that the length of the Bloch vector $|\langle \mathbf{J} \rangle|$ is only slightly reduced.

The atoms are trapped inside an optical cavity tuned to resonance with the $|\uparrow\rangle$ to $|e\rangle \equiv |5^2P_{1/2}, F = 1, m_F = 0\rangle$ optical transition with wavelength $\lambda = 795$ nm [see Fig. 2(b)]. To account for lattice sites where atoms only

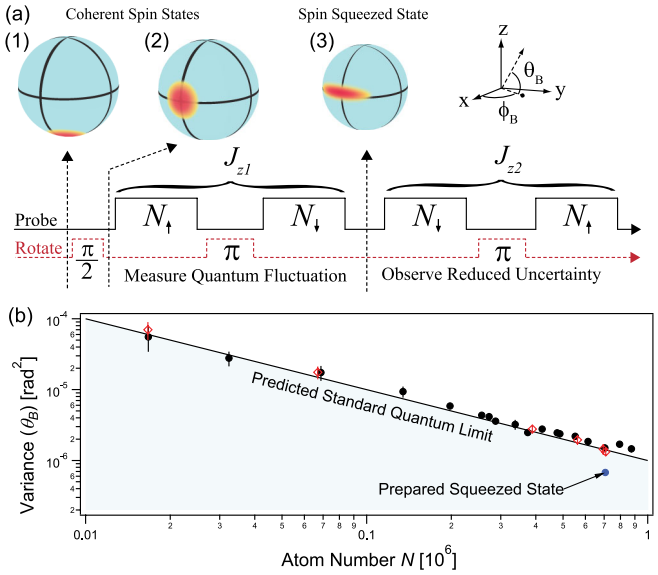

FIG. 1 (color online). (a) The quantum noise of a collection of pseudospin $\frac{1}{2}$ atoms can be represented as a classical probability distribution for the collective spin or Bloch vector with length $J_{\max} = N/2$. Probing the number of atoms in spin up and spin down measures the projection $J_z = (N_\uparrow - N_\downarrow)/2$, as well as $J_{\max}$. For states near the equator, the polar angle is $\theta_B \approx J_z/J_{\max}$. The population measurement sequence consists of composite microwave rotations (dashed line) and QND population measurements (solid line). The evolution of the ensemble is represented by Bloch spheres 1, 2, and 3. The QND measurement projects the ensemble into a conditionally squeezed state (3), which is verified with the second measurement. (b) The observed variance of θ_B versus atom number confirms the predicted standard quantum limit. Two different rotations (circles and diamonds) are used to constrain added noise from the rotations [21].

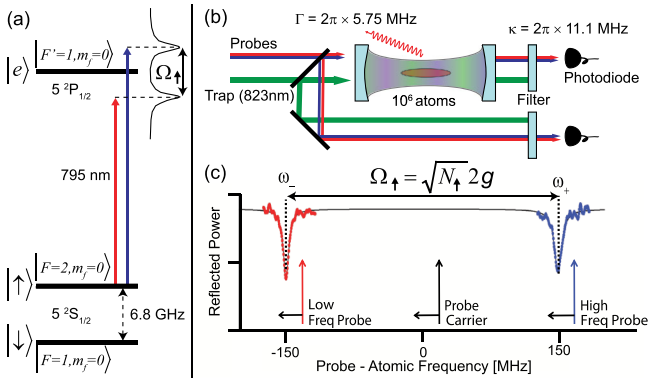

FIG. 2 (color online). (a) The clock states $|\uparrow\rangle$ and $|\downarrow\rangle$ form a pseudospin-$\frac{1}{2}$ system. The population $N_\uparrow$ is measured by probing near the $|\uparrow\rangle$ to $|e\rangle$ transition, which couples to a degenerate cavity mode, creating a collective vacuum Rabi splitting $\Omega_\uparrow$. (b) An ensemble of 10^6 atoms are tightly confined within the TEM_{00} mode using a 1D intracavity optical lattice at wavelength 823 nm. The cavity power and atomic population decay rates are κ and Γ, respectively. A heterodyne interferometer (not shown) is used to probe the atom-cavity resonances. The collective nature of the Rabi splitting prevents loss of coherence as atoms remain in a superposition after the measurement. (c) The vacuum Rabi splitting $\Omega_\uparrow = \omega_+ - \omega_-$ is measured by simultaneously scanning the probe frequencies across the upper and lower atom-cavity resonances $\omega_\pm$. The size of the fitted splitting determines the population in $|\uparrow\rangle$ from $N_\uparrow = (\Omega_\uparrow/2g)^2$. A single scan requires ≈ 70 μs.

weakly couple to the probe mode, we follow the procedure of Ref. [17] by defining effective parameters, N and g, such that $\Delta J_{z\mathrm{CSS}}$ remains $\sqrt{N}/2$ [21]. The effective single particle vacuum Rabi frequency is $2g = 2\pi \times 506(8)$ kHz [21]. Coupling to the cavity mode is enhanced by using up to $N = 7 \times 10^5$ so that the collective cooperativity parameter $N_\uparrow C \approx 1400$ is large.

The atomic population is determined from $N_\uparrow = (\Omega_\uparrow/2g)^2$, where $\Omega_\uparrow$ is the collective vacuum Rabi splitting [22]. The bare cavity mode is dressed by the presence of atoms in state $|\uparrow\rangle$ to generate two new resonances at frequencies $\omega_\pm$ relative to the original cavity resonance [see Fig. 2(c)]. The measured splitting $\Omega_\uparrow = \omega_+ - \omega_-$ is only quadratically sensitive to detuning between the atomic and bare cavity resonances, relaxing technical requirements on cavity stability. Requirements on laser frequency stability are also relaxed by simultaneously scanning the resonances using two probe frequency components generated by phase modulating a single laser.

The other population $N_\downarrow$ is determined by first applying a microwave π pulse that phase coherently swaps the populations between $|\downarrow\rangle$ and $|\uparrow\rangle$ [see Fig. 1(a)]. The population of $|\uparrow\rangle$ is then determined from the vacuum Rabi splitting with the results labeled $N_\downarrow$ and $\Omega_\downarrow$. For scale, the predicted projection noise $\Delta J_{z\mathrm{CSS}}$ would produce rms fluctuations in the vacuum Rabi splittings of $\Delta(\Omega_\uparrow - \Omega_\downarrow) = \sqrt{2}g = 2\pi \times 358(6)$ kHz.

The predicted projection noise variance $(\Delta J_{z\mathrm{CSS}})^2$ is confirmed to 2(6)% by measurements of the variance of J_{z1} versus atom number [see Fig. 1(b)]. Projection noise results in a linear dependence of the variance with atom number, whose magnitude is determined using low order polynomial fits. The fitted linear contribution is $1.02 \pm 0.05(\mathrm{stat}) \pm 0.04(\mathrm{syst})$ times $(\Delta J_{z\mathrm{CSS}})^2$.

We now demonstrate that repeated measurements of J_z are correlated below the projection noise level $\Delta J_{z\mathrm{CSS}}$. A first measurement J_{z1} estimates J_z to a precision set primarily by the measurement noise ΔJ_{zm}, preparing a subprojection noise state when $\Delta J_{zm} < \Delta J_{z\mathrm{CSS}}$. As shown in Fig. 3, quantum projection noise plus added classical and detection noise causes fluctuations in the measured J_{z1} from one trial to the next, but the fluctuations are partially correlated with a second measurement J_{z2}, allowing the quantum noise to be partially canceled in the difference $J_{z2} - J_{z1}$.

At $N_0 = 7.0(3) \times 10^5$ atoms and a probe photon number of $M_0 = 1.9(1) \times 10^5$ per measurement of J_z, the variance of the difference of two QND measurements was $(\Delta(J_{z2} - J_{z1}))^2/(\Delta J_{z\mathrm{CSS}})^2 = -2.6(3)$ dB, where a Bayesian estimator for J_{z1} was applied. Subtracting the measurement noise ΔJ_{zm} of the second measurement in quadrature gives a conservative estimate of the uncertainty in J_z after the first QND measurement of $(\Delta J_z)^2/(\Delta J_{z\mathrm{CSS}})^2 = -4.9(6)$ dB. The noise ΔJ_{zm} is determined from fluctuations in the difference of two time

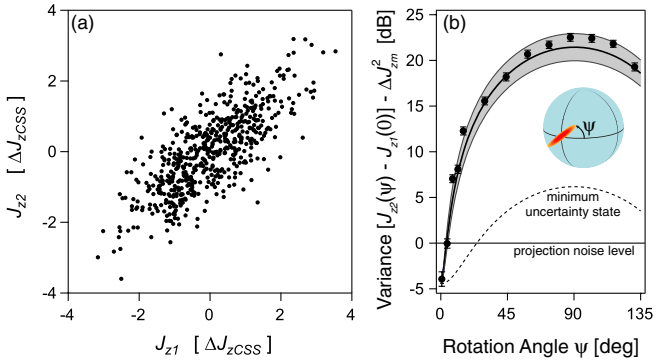

FIG. 3 (color online). (a) The first and second QND measurements of J_z exhibit correlated fluctuations that arise largely from projection noise. (b) The noise in the backaction quadrature is observed by inserting a rotation through angle ψ between the QND measurements J_{z1} and J_{z2}. The dashed curve is the calculated response for a minimum uncertainty squeezed state, while the solid curve with the gray 68% confidence interval is the predicted backaction from the intracavity probe vacuum noise.

adjacent $N_\downarrow$ measurements [21]. Accounting for fluctuations in Raman scattering to other magnetic sublevels does not change this result.

The unmeasured azimuthal angle ϕ_B is driven by fluctuating ac stark shifts arising from the intracavity probe vacuum noise [see Fig. 3(b) and Ref. [23].] The measured and predicted quantum backaction noise levels are 22.3(1) and 21.4(1.5) dB relative to projection noise, respectively. The backaction is larger than that of a minimum uncertainty squeezed state due to finite quantum and technical efficiencies in the probe detection process.

Reduction of spin noise alone does not allow improved quantum phase estimation unless the length of the Bloch vector $|\langle \mathbf{J} \rangle|$ is sufficiently unchanged. The normalized length of the Bloch vector is measured by varying the polar angle θ_B from 0 to 2π and determining the contrast $\mathcal{C} = |\langle \mathbf{J} \rangle|/J_{\max}$ from the resulting variation of the population $N_\uparrow$ (see Fig. 4). Before the QND measurements, the contrast is $\mathcal{C}_i = 0.97(1)$, and the first QND measurement reduces the contrast to $\mathcal{C}_f = 0.82(2)$.

Free space scattering of probe photons leads to collapse of the spin wave function of individual spins and is the dominant source of decoherence. A rate equation analysis predicts the number of probe photons scattered into free space M_{sc} is related to the total number of probe photons M by $M_{\mathrm{sc}}/M = 0.41(1)$. This prediction is in excellent agreement with the measured value 0.41(2) deduced by measuring the decrease in the vacuum Rabi splitting due to Raman scattering versus probe photon number. If each scattered photon leads to the collapse of a single spin, then the fractional reduction in contrast is $6.4(3) \times 10^{-7} \times M$ at N_0 atoms. As shown in Fig. 4, the measured contrast versus probe photon number is well described by $\mathcal{C}_f = \mathcal{C}_i - k_1 M - k_2 M^2$. The fitted value, $k_1 = 5.5(7) \times 10^{-7}$ per photon, is in good agreement with the prediction and

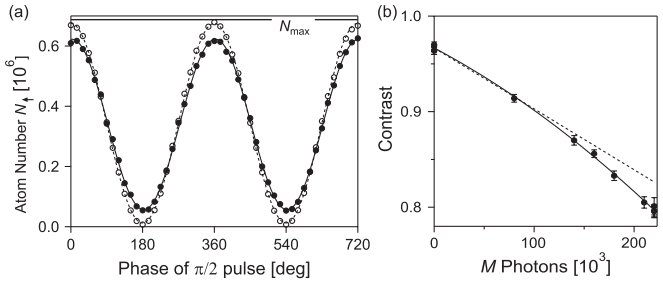

FIG. 4. (a) The degree of coherence remaining after the measurement J_{z1} is determined using the sequence: $(\frac{\pi}{2})$–(measure $N_\uparrow$)–(π)–(measure $N_\downarrow$)–$(\frac{\pi}{2})$–(measure $N_\uparrow$). The sequence is repeated and the final measured value of $N_\uparrow$ is plotted versus the phase of the final $\frac{\pi}{2}$ pulse. With no measurements (empty circles), the background contrast is $\mathcal{C}_i = 0.97(1)$. Probing with 1.8×10^5 photons (filled circles), causes a small reduction in contrast despite a measurement sensitivity below the projection noise level. (b) Measured contrast versus probe photon number (solid circles), second order polynomial fit (solid line), and the predicted contrast loss due to free space scattering alone (dashed line).

confirms the fundamental role of free space scattering as the dominant source of decoherence.

The quadratic variation of $\mathcal{C}_f$, $k_2 = 1.0(3) \times 10^{-12}$ per (photon)^2, arises from uncanceled inhomogeneous probe-induced light shifts that result in dephasing of the ensemble. These light shifts are largely spin echoed away with the π pulse used to measure J_{z1}. The uncanceled dephasing arises from radial motion in the trap. At fixed measurement precision, the magnitude of the dephasing increases linearly with probe detuning, making it easier to reach a scattering-dominated regime in this work compared to work in a far-detuned dispersive regime [17].

The ability to estimate the polar angle $\theta_B \approx J_z/|\langle \mathbf{J} \rangle|$ is largely set by the noise in J_z and the signal size $|\langle \mathbf{J} \rangle|$. From Ref. [20], the directly observed spectroscopic gain is given by $\zeta_m^{-1} = \mathcal{C}_f^2(\Delta J_{z\mathrm{CSS}})^2/(\mathcal{C}_i(\Delta(J_{z2} - J_{z1}))^2) = 1.1(4)$ dB below the standard quantum limit. We infer the ability to prepare states with enhanced spectroscopic sensitivities of $\zeta_m^{-1} = \mathcal{C}_f^2(\Delta J_{z\mathrm{CSS}})^2/(\mathcal{C}_i(\Delta J_z)^2) = 3.4(6)$ dB.

The coherence-preserving nature of these measurements can be contrasted with that of weak, sampled measurements such as fluorescence detection of an optically thin ensemble. The angle θ_B could be estimated by extracting 15% of the initially undecohered atoms, and performing perfect state detection on this subensemble. The loss of signal would be the same as observed in our experiment, but the subensemble's estimate of θ_B would be $G = 13(1)$ dB noisier than the precision demonstrated using a collective measurement approach. This reduction in noise can be described as arising from a noiseless amplifier of gain G placed before a 15/85 atom beam splitter [24].

In the future, this method can be extended to achieve greater violations of the standard quantum limit since many experimental aspects, such as cavity finesse and length, can be easily improved. Running wave cavities or commensurate optical lattices can be employed to create squeezed states appropriate for launching ensembles into free space for matter wave interferometry.

We thank V. Vuletić and J. Simon for interesting discussions, A. Hati, D. Howe, K. Lehnert, and L. Sinclair for help with microwaves, and H. S. Ku, S. Moses, and D. Barker for early contributions. This work was supported by the NSF AMO PFC and NIST. Z. C. acknowledges support from A*STAR Singapore.

[1] A. D. Ludlow *et al.*, Science **319**, 1805 (2008).
[2] T. L. Gustavson, P. Bouyer, and M. A. Kasevich, Phys. Rev. Lett. **78**, 2046 (1997).
[3] P. J. Mohr, B. N. Taylor, and D. B. Newell, Rev. Mod. Phys. **80**, 633 (2008).
[4] A. Wicht *et al.*, Phys. Scr. **T102**, 82 (2002).
[5] A. André, A. S. Sørensen, and M. D. Lukin, Phys. Rev. Lett. **92**, 230801 (2004).
[6] M. Auzinsh *et al.*, Phys. Rev. Lett. **93**, 173002 (2004).
[7] T. P. Heavner *et al.*, Metrologia **42**, 411 (2005).
[8] J. Lodewyck, P. G. Westergaard, and P. Lemonde, Phys. Rev. A **79**, 061401 (2009).
[9] D. Leibfried *et al.*, Science **304**, 1476 (2004).
[10] V. Meyer *et al.*, Phys. Rev. Lett. **86**, 5870 (2001).
[11] T. Monz *et al.*, arXiv:1009.6126.
[12] J. Estève *et al.*, Nature (London) **455**, 1216 (2008).
[13] C. Gross *et al.*, Nature (London) **464**, 1165 (2010).
[14] M. F. Riedel *et al.*, Nature (London) **464**, 1170 (2010).
[15] A. Kuzmich, N. P. Bigelow, and L. Mandel, Europhys. Lett. **42**, 481 (1998).
[16] J. Appel *et al.*, Proc. Natl. Acad. Sci. U.S.A. **106**, 10 960 (2009).
[17] M. H. Schleier-Smith, I. D. Leroux, and V. Vuletić, Phys. Rev. Lett. **104**, 073604 (2010).
[18] W. Wasilewski *et al.*, Phys. Rev. Lett. **104**, 133601 (2010).
[19] I. D. Leroux, M. H. Schleier-Smith, and V. Vuletić, Phys. Rev. Lett. **104**, 073602 (2010).
[20] D. J. Wineland, J. J. Bollinger, W. M. Itano, and D. J. Heinzen, Phys. Rev. A **50**, 67 (1994).
[21] See supplemental material at http://link.aps.org/supplemental/10.1103/PhysRevLett.106.133601 for experimental details.
[22] Y. Zhu *et al.*, Phys. Rev. Lett. **64**, 2499 (1990).
[23] I. Teper, G. Vrijsen, J. Lee, and M. A. Kasevich, Phys. Rev. A **78**, 051803 (2008).
[24] P. Grangier, J. A. Levenson, and J.-P. Poizat, Nature (London) **396**, 537 (1998).